UCRL-17456

University of California

Ernest O. Lawrence Radiation Laboratory

SMALL ANGLE X-RAY SCATTERING AND LOW ENERGY ELECTRON DIFFRACTION STUDIES OF CATALYST SURFACES

TWO-WEEK LOAN COPY

This is a Library Circulating Copy which may be borrowed for two weeks. For a personal retention copy, call Tech. Info. Division, Ext. 5545

DISCLAIMER

This document was prepared as an account of work sponsored by the United States Government. While this document is believed to contain correct information, neither the United States Government nor any agency thereof, nor the Regents of the University of California, nor any of their employees, makes any warranty, express or implied, or assumes any legal responsibility for the accuracy, completeness, or usefulness of any information, apparatus, product, or process disclosed, or represents that its use would not infringe privately owned rights. Reference herein to any specific commercial product, process, or service by its trade name, trademark, manufacturer, or otherwise, does not necessarily constitute or imply its endorsement, recommendation, or favoring by the United States Government or any agency thereof, or the Regents of the University of California. The views and opinions of authors expressed herein do not necessarily state or reflect those of the United States Government or any agency thereof or the Regents of the University of California.

Submitted to: Eastern Analytical Symposium Series

UCRL-17456
Preprint

UNIVERSITY OF CALIFORNIA
Lawrence Radiation Laboratory
Berkeley, California

AEC Contract No. W-7405-eng-48

SMALL ANGLE X-RAY SCATTERING AND LOW ENERGY ELECTRON DIFFRACTION STUDIES OF CATALYST SURFACES

Gabor A. Somorjai

March 1967

SMALL ANGLE X-RAY SCATTERING AND LOW ENERGY ELECTRON DIFFRACTION STUDIES OF CATALYST SURFACES

Gabor A. Somorjai

Inorganic Materials Research Division, Lawrence Radiation Laboratory,
Department of Chemistry, University of California,
Berkelely, California

I. INTRODUCTION

Studies of solid surfaces and chemical reactions which occur at the interface are among the most important and exciting fields of chemistry. The abundance and variety of surface catalytic processes indicate the diversity of roles the solid surface seems to play during the reaction. The largest obstacle however, which prevents closer scrutiny of the structure of surfaces and the detailed mechanism of a surface reaction, has been the scarcity of experimental tools which permit one to study surface properties on an atomic scale.

Low energy electron diffraction (LEED) proves to be a novel experimental technique which permits the study of the structure and rearrangements of atoms in the surface plane. Since the electrons do not penetrate below a few atomic planes (four-five) the diffraction patterns are representative of the surface arrangement of atoms. Thus, this technique is sensitive only to surface properties. Low energy electron diffraction plays the same role in analyzing the structure of solid surfaces as x-rays in studies of the bulk structure. The technique can also be employed for studies of the structure of adsorbed gases and for investigations of chemical surface reactions.

There is also widespread use of polycrystalline metal particles of size 10Å - 10^3Å in catalytic surface reactions which are dispersed on

highly porous supports. Typical supported catalysts include platinum, palladium, or nickel supported on alumina or silica. There has been a lack of effective experimental techniques which allow studies of the sizes, shapes of such particles and their changes which occur during chemical reactions. Changes in particle size, i.e. in the surface to volume ratio can markedly influence the rates of catalytic surface reactions.

Small angle x-ray scattering proves to be the most versatile technique to detect and monitor particles ranging from 40Å to 600Å. The only criterion for monitoring the changes which effect the particle shape or size in this range is the presence of an electron density difference between the metal particles to be investigated and the support matrix, since the scattered intensity is proportional to the square of the difference in electron density.[1]

In this paper we shall discuss two studies of platinum surfaces; 1) A low energy electron diffraction study of the clean (100), (111), and (110) faces of platinum single crystals, and 2) A small angle x-ray scattering investigation of the effect of thermal history on the particle size of platinum catalysts dispersed on highly porous η-alumina.

These studies should give indication of the types of experimental information which could be obtained by these techniques.

II. PRINCIPLES OF LOW ENERGY ELECTRON DIFFRACTION

In low energy electron diffraction studies one uses monochromatic electrons of energies $E \approx 5\text{-}500 \pm 0.2$ev, which correspond to a wavelength range of roughly 0.5-5Å. $\lambda(\text{Å}) = [150/E(\text{eV})]^{1/2}$. The most versatile low energy electron diffraction apparatus for catalytic studies seems to be the post-acceleration type (Varian Associates, Palo Alto, Calif.). The schematic representation of the experiment is shown in Fig. (1). The electrostatically focused electrons (≈1μamps) are back reflected from the crystal surface due to their charge and large mass. The crystal and the first grid are at ground potential to assure a field-free region in order to minimize distortion of the path of the scattered electrons. The second grid serves to retard the inelastically scattered fraction of electrons and it is held generally at cathode potential. The elastically scattered electrons, which contain the diffraction information, penetrate the second grid, are accelerated and strike a fluorescent screen where the diffraction pattern which corresponds to the surface structure is displayed. Although better focusing[2] and energy selection[3] techniques have been reported which could give almost an order of magnitude better resolution with some sacrifice of the beam intensity, the electron optics which are described above proved to be entirely adequate for catalytic surface reaction studies.

Our studies on platinum surfaces indicate that in the range 20-50 eV the diffraction is essentially two dimensional. Above this energy two to five atomic planes seem to contribute to the diffraction. The surface structures which are the property of the topmost layer of atoms are visible in the energy range 5-150 eV. At higher energies electrons penetrate deeper below the surface and the relative contribution of atoms in the

surface plane to the total scattered intensity diminishes.

The scattering amplitude of electrons by atoms is approximately three orders of magnitude greater than that of x-rays.[4] This implies a six order of magnitude greater scattered intensity. Thus electrons are so efficient scatterers that only a small concentration of surface atoms which are ordered in regular arrays are needed to give detectable diffraction patterns. Patterns which are due to atomic arrangements occupying less than 5% of the total number of surface sites (~5% coverage) have been detected.(5) The surface domains which give rise to the diffraction patterns contain on the average 40 atoms in ordered arrays.[6] The observed intensities come from the coherent superposition of electron waves scattered by these separate domains.

Due to the large scattered intensity there is no need for detection techniques which are accumulative in a long time span. Thus, visual or photographic detection of the diffraction patterns which are displayed on the fluorescent screen is sufficient. The intensity changes of the diffraction spots can be monitored by a high sensitivity, small angle spectrophotometer (Gamma Optical Co., Model 2000 was used in these studies).

The fraction of elastically scattered electrons is 5-10% in the energy range 100-450 eV.[5] At lower electron energies the fraction of electrons which are back-reflected without energy loss increases sharply and attains the 50-80% range at 20 eV. Thus, the surface becomes highly reflective for low energy electrons.[5]

The lateral coherence length of electrons, using the commercially available electron optics is ≈ 15-20Å. Since this is appreciably smaller

than the average domain size (~40 atoms ~120Å), direct detection of atomic steps is difficult.[6]

In low energy electron diffraction studies one face of a high purity single crystal of size appreciably larger than that of the size of the electron beam (1 mm^2) should ideally be used. The experiment is carried out in vacuum of better than 10^{-8} torr in order to avoid surface contamination due to adsorbed gases. A crystal surface will adsorb a monolayer of foreign gas at 10^{-6} torr in about one second (assuming a sticking coefficient of unity) so that typical operating pressures in the diffraction chamber are 10^{-8} to 10^{-10} torr to allow reasonable observation times of the clean surface. The diffraction apparatus and the high vacuum system which are necessary for these surface studies are available commercially at a reasonable cost.

The use of a mass spectrometer which can be attached to the diffraction chamber is necessary for studies of chemical surface reactions. The availability of quadrupole mass spectrometers in recent years (Electronic Associates Model 210 was used in our studies) which are compact and have high detection sensitivity (10^{-12} torr partial pressure) have aided greatly the definitive interpretation of the experimental results. The mass spectrometer allows one to monitor changes in the mass spectrum which are caused by less than 1% of the monolayer provided that the desorption takes place in short times (about one minute). The use of a mass spectrometer can also greatly aid the detection of surface contaminants.

The single crystal surface area on which the studied chemical surface reaction takes place is much smaller than the wall area of the diffraction chamber. Care should be taken therefore that the reactants and the reaction products do not undergo chemical changes when colliding with the wall of the chamber. If the reaction which is to be studied is

influenced by collisions with the chamber wall the experiment could be designed to assure that the reactant gas species impinge directly onto the surface of the single crystal and that the product species can enter the ionizer region of the mass spectrometer without colliding with the chamber walls first.

Low energy electron diffraction studies of solid single crystal surfaces have revealed a great deal of information about the physical-chemical properties of surface which could not have been obtained by other experimental techniques.[5] One of the striking results of low energy electron diffraction studies on clean solid surfaces is the discovery that the substrate atoms may reside in surface structures of different kind.[7] The presence of these surface structures is indicated by the appearance of extra diffraction features which are superimposed on the diffraction pattern of the substrate unit mesh predicted by the bulk unit cell. One can assign lattice parameters to these surface structures which, in general, were found to be integral multiples of the lattice parameters which characterize the substrate. Studies on clean semiconductor and metal surfaces have revealed the presence of several surface structures with unit cells in the range of twice (2X2) or as large as eight times (8X8) the unit cell dimensions of the substrate.[5,8] The exact arrangement of atoms which produce these structures is still in question. Their appearance, however, indicates a) long range order on the surface, and b) that transformation (reversible or irreversible) from one type of surface structure to another can readily occur. Thus, these structures which may be called surface phases have a temperature range of stability, and phase transformations at the surface can take place without any apparent effect on the bulk structure.

There are several reasons for the existence of surface structures which are indicated by recent experiments.[5] The activation energy for surface diffusion of adatoms is appreciably smaller than either the activation energy for bulk diffusion or the heat of sublimation in monatomic solids.[9] Thus, surface atoms are shielded by large potential energy carriers from rapid exchange with the bulk or vacuum. The phonon spectrum of surface atoms is different from that of the bulk atoms as shown by surface Debye temperature measurements.[10,11] There is also some experimental evidence that, in addition to the change in the mean square displacement of atom at the surface, there is a net expansion or contraction with respect to the bulk lattice spacing.[12,13]

Another striking discovery of low energy electron diffraction studies is the observation that adsorbed gases form a variety of ordered surface structures on the different solid surface.[5] The type of structure which forms depends on the crystallographic orientation and temperature of the substrate and the size, surface concentration and chemical nature of the adsorbed species. Structural transformations easily occur as a function of changes in these parameters. Consequently a great wealth of surface structures which can be attributed to the adsorbed species have already been reported.[5]

These experimental results seem to indicate that a study of surface structures which are due to the solid atoms or to adsorbed gas atoms is essential to understand the nature of catalytic surface reactions. It is already apparent that the diversity of surface catalytic properties can be correlated with the variety of surface phases and structures which seem to form as a function of experimental conditions. Low energy electron diffraction can provide us with such structural information.

III. LOW ENERGY ELECTRON DIFFRACTION STUDY OF THE (100), (111), AND (110) FACES OF PLATINUM

A. Experimental

Platinum single crystals of the highest purity (99.9999%) were used in the experiments. The samples (0.5 to 2 mm thick and 6 mm in diameter) were cut after orienting the particular face by x-ray within one degree. The crystals were then polished, etched, and spotwelded to a platinum holder. After spotwelding thermocouples to the back of the crystal, the sample was introduced into the diffraction chamber. Baking and degassing the evacuated diffraction chamber produced pressures of the order of $5X10^{-10}$ torr.

Ion bombardment using high purity xenon or argon was employed in order to a) remove the surface damage which was caused by the mechanical surface treatments, or b) remove disordered surface structure which formed irreversibly at high temperatures ($T > 750°C$). Usual conditions of ion sputtering were $2X10^{-5}$ torr A or Xe, 340 eV accelerating potential for two hours. Heating the samples to $T \lesssim 900°C$ has also produced diffraction features without ion bombardment. At these elevated temperatures, however, the ring-like diffraction patterns which are characteristic of the disordered surface structure formed irreversibly and therefore studies of the platinum surface structures which are present at lower temperatures could not be made. Thus, ion bombardment and subsequent heat treatment was necessary to generate the clean substrate structure or the low temperature surface structures. All of the surface structures reported in this paper were reproducible under all conditions of surface preparations and ion bombardment treatments unless otherwise noted.

In order to monitor the composition of the ambient and detect the presence of possible surface contaminants a quadrupole mass spectrometer (EAI 210) was permanently mounted on the diffraction chamber. This way we

could continuously monitor the background ambient composition during heat treatments and the composition of the gases used for ion bombardment.

In order to further probe the nature of the different surface structures, they were heated in oxygen and in hydrogen in their temperature range of stability. In this manner, surface contaminants which form volatile oxide produces or react in a reducing atmosphere could be detected by the mass spectrometer and eliminated from the surface.

The diffraction patterns yield a great deal of information as to the structures of the surface. Intensity analysis of the diffraction features is necessary, however, to distinguish between several structures which could yield similar diffraction patterns.[5] This is carried out by monitoring the intensity of the diffracted beam as a function of electron energy and scattering angle. Variation of the intensity of a given diffraction spot with heat treatment or in the presence of gases can give information on the kinetics of surface diffusion or adsorption. Intensity measurements were made using a telephotometer with fiber optics (Gamma Scientific Instruments, Model 2000) which allowed highly reproducible measurements of intensity fluctuation with beam voltage which were plotted on an x-y recorder. These were then taken at various angles of incidence. The fluorescent screen has also been photographed directly to obtain the diffraction patterns. The relative intensities could then be obtained by using a densitometer.

B. Surface Phase Transformations as a Function of Temperature

Annealing the crystals at 600°C for one hour after the ion bombardment has produced the diffraction patterns which are predicted by the bulk unit cell. Using the notation that is suggested by Wood, this corresponds to the (1X1) or substrate structure.

If the samples are annealed after ion bombardment in other temperature ranges, either below or above 600°C, new diffraction spots appear which indicate that the atoms at the surface are arranged in surface structures which are different from that predicted by the bulk unit cell. These surface structures can be easily reproduced on all of the single crystal sample used. All of the structures which were observed on the different platinum substrates are summarized in Table I. The structures are divided into two types, ordered and disordered. The ordered surface structures are stable only at temperatures roughly below one-half the melting temperature and characterized by unit cells which are integral multiples of the substrate unit cell. The disordered structures appear at high temperatures. All of the experimental observations seem to indicate that both types of surface structures are the property of the clean platinum surfaces. No single impurity produces the variety of diffraction features which were observed as a function of substrate temperature in the high purity platinum surfaces. The surface structures show a broad range of different physical properties (stability range, long or short range order, different types of surface structures on each substrate). Heat treatment in ultrahigh vacuum, in oxidizing or reducing ambients, has not produced any new volatile species which could be detected by the mass spectrometer.

1. Properties of the Ordered Surface Structures

The following statements summarize the experimental information concerning the ordered surface structures which appear on the different platinum substrates.

a. The surface structures which appear on the different crystal faces of platinum are stable only in well defined temperature ranges. The stability range of two structures may overlap on the given substrate.

b. The surface structures are not affected by heat treatments in oxygen or hydrogen in their temperature range of stability.

c. The structures are in registry with the substrate (not rotated) and are characterized by lattice parameters which are integral multiples of that of the substrate [(5X1), (2X1), (2X2), (3X3)].

d. The surface structures anneal out at temperatures below their range of stability but reappear readily when reheated in their stability range. Once heated above this temperature range they disappear irreversibly.

e. The surface structures were obtained only after ion bombardment. The properties of the surface structures, however, were independent of the type of ions which were used in the ion bombardment.

f. The surface structures could rapidly be obtained by applying a steep temperature gradient along the gradient surface. The structures could also be formed on the (100) substrate by heating the crystals in a well-defined temperature range.

g. The intensity of the diffracted beams emanating from the surface structures is of the same order of magnitude as the intensity of the substrate reflections.

h. The different heat treatments have not resulted in any appreciable rise in the ambient pressure or in the appearance of volatile impurities, either when the heating was commenced or during the heating period.

i. The presence of these surface structures causes no change in the positions of the intensity maxima in the I_{00} vs. E(eV) curves which were taken for the clean substrates.

j. Several surface structures were found to exist on the (100)-face of silver, gold, and palladium single crystals.[14,15] The ordered surface structures on the gold substrate are similar to those found on the (100)-face of platinum.

2. Properties of the Disordered Surface Structures

When the (100) substrate was heated above 700°C a new diffraction pattern slowly appears. This is characterized by narrow, circular segments. Six such segments appear at first, then with increased heating time or high heating temperature, 12 and then 24 segments form which finally join into a ring.

The ring-like patterns can be obtained without ion bombardment, only by heating the sample between 700°C and the melting temperature (1769°C). Their formation is irreversible, i.e., once they have been created they are stable indefinitely at any temperature below the melting point and can only be removed by ion bombardment.

If the sample is heated above 1000°C for an extended period (4-6 hours), the intensity of the diffraction features which are due to the substrate unit mesh and which coexist with the ring pattern decreases while the intensity of the rings increases. When heated near the melting point, the ring-like diffraction pattern finally remains the only diffraction feature on a presumably greatly disordered surface.

The rings are concentric about the (00)-reflection, have sharp outlines and show the usual diffraction features of other surface structures, (a) appear only at low electron energies (5-150 eV) and (b) appear at decreasing angles with respect to the (00)-spot with increasing electron energy. One striking feature of the ring pattern is that it does not overlap with any of the diffraction spots which are due to the substrate unit mesh.

Ring-like diffraction patterns were also found to exist on both the (111) and (110) platinum surfaces as well.

The following statements summarize some of the important properties

of the disordered surface structures and other pertinent information which could be used to interpret these structures.

a. Ring-like diffraction patterns form on the (111), (110), and (100) substrates of platinum via sets of radially symmetric segements at elevated temperatures.

b. Their formation is irreversible and they become the only diffraction feature of the surface as the melting point is approached. They may be formed without the use of ion bombardment, by heating the substrate in their temperature range of stability.

c. The ring patterns are unaffected by heat treatment in hydrogen or oxygen atmospheres.

d. The rings appear to have apparent lattice parameters which are smaller than the smallest interplanar distance in the substrate plane.

e. The surface structure which gives rise to the ring pattern is parallel to the surface upon which it forms and shows diffraction features similar to other surface structures.

f. The ring-like patterns are narrow and well-defined and always appear in the same position on a given substrate. They are unlike the radial distribution functions observed by neutron diffraction[16] or x-ray diffraction studies of liquids near the melting point.[17]

g. The formation of these ring patterns reflects the gradual loss of long range order at the surface as heating time or temperature is increased.

h. Ring-like diffraction patterns were also found to form on other metal surfaces.[14,15] They have apparent lattice dimensions which are smaller (Ir, Au) or larger (Ag) than the distance of closest approach in the ordered substrate.

i. There is no evidence of any macroscopic change in the surface structure of platinum as observed in the photomicrograph (1000 X magnification)

when the ring-like diffraction pattern is formed.

The lattice parameters and the same ratio of lattice spacings which can be assigned[18] to the different rings ($d_0^I/d_0^{II} = \sqrt{3}$ and $d_0^I/d_0^{III} = 2$) on all three substrates suggest that the ring-like diffraction patterns are due to domains of (111) surface structures on all faces of platinum with reduced nearest neighbor spacing. These hexagonal surface structures appear at preferred orientations at first as shown by the presence of ring segments. After extended heating time or as the melting temperature is approached they can be freely rotated in the substrate plane. The disordered hexagonal surface structures show an 11% contraction with respect to the interplanar spacings in the ordered (111) face.

In addition to the ring-like patterns on the platinum surfaces, ring or segmented ring-like surface structures have been observed on gold (100), silver (100), and iridium (111) surfaces.[14,15] In no case do the diffraction rings coincide with the diffraction spots of the substrate, but show "contraction" or "expansion" of different magnitudes. For example, in silver the apparent lattice parameter which can be assigned to the ring pattern indicates a 13% expansion with respect to the nearest neighbor distance in the ordered substrate while gold shows a "contraction" which is similar to that of platinum. It is likely that the disordered phase is present at high temperatures on many face centered cubic metal surfaces which have low enough evaporation rate not to permit the removal of the new phase into the vapor as soon as it forms.

IV. PRINCIPLES OF SMALL ANGLE X-RAY SCATTERING

The small angle x-ray measurements were made using CuK_α radiation, a four-slit collimating system and a sample-detector distance of 50 cm. Figure (2) shows a schematic representation ~~of the instrumental~~ arragement. Although this apparatus was built in our laboratory, several small angle x-ray scattering attachements are available commercially which assures easy applicability of this technique. The sample was mounted on a one-mil Mylar sheet behind the third slit. The x-ray intensity was measured using scintillation counting with pulse height selection.[19,20]

The smallest angle which did not strike the primary beam was 0.0733 degrees, or about 4.4 minutes of arc. The largest angle at which these experiments gave scattering intensity distinguishable from the background was about 1.1 degrees. Roughly these angles correspond to particles ranging from 40Å to 600Å.

The pulses leaving the analyzer (10) were counted with a conventional scale-of-256 and a mechanical register. The typical counting rate was some 2000 pulses per minute, although it was much higher near the primary beam and much lower at angles near one degree.

From the small-angle x-ray scattering, the datum that can be calculated most directly is the average radius of gyration of the scattering particles. For a detailed discussion of the theory, the reader is referred to Guinier's book.[1]

The scattering intensity i(h) for N noninteracting particles is given as

$$i(h) = i_e(h)N\overline{F^2(h)} \qquad (1)$$

where $i_e(h)$ is the intensity of scattering by one electron, F(h) is the structure factor, and $h = (4\pi/\lambda) \sin \theta$, where λ is the x-ray

wavelength and 2 θ is the scattering angle. At small angles F(h) is approximated by $\overline{F^2(h)} = n^2 \exp(-h^2 r^2/3)$ where r is the radius of gyration and n is the total number of electrons in the particle. For small angles $[(4\pi/\lambda) \sin \theta \simeq (4\pi/\lambda)\theta]$, r is given by

$$r = \frac{1}{2\pi} \sqrt{\frac{3}{\log_{10} e}}\, \lambda \sqrt{p} \qquad (2)$$

where p is the negative slope of the log i(h) vs. $(\tan 2\theta)^2$ curve. In case of the CuKα radiation $r(\mathring{A}) = 0.645 \sqrt{p}$.

The usual plot for obtaining the average radius of gyration is therefore the Guinier plot, log i vs. h^2, where h is proportional to the angle: $h = (2\pi/\lambda) \tan 2\theta \simeq 4\pi\lambda^{-1}\theta$. The slope gives the desired radius. However, the initial slope must be used, because at larger angles the Guinier exponential approximation begins to fail.

In interpreting the scattering results of this investigation, the Guinier plot was used to determine the average radii of the platinum particles.

A. Particle Shape and Size Distribution

For spherical or nearly spherical particles the Guinier approximation holds best. However, there is no "built-in" shape factor in the integral. Furthermore, most of the systems to be investigated by means of small-angle x-ray scattering are heterodisperse, and the distribution of particles is of great interest. Shull and Roess[21] developed a method for calculating small-angle scattering intensities of heterodisperse systems, inserting a distribution function into the scattering integral. It was assumed that all particles are geometrically similar; that is, the number of electrons n is proportional to r, where r is the radius of gyration.

Then

$$i(h) = K \int_0^\infty \overline{F^2(h)} N(r) r^6 dr \qquad (3)$$

where N(f) is the number distribution function and N(r) dr represents the total number of particles in thr size range r, r + dr. K is constant. The exact structure factor for spheroids,

$$\overline{F^2(h)} = 9\left(\frac{\sin rh - rh \cos rh}{r^3 h^3}\right)^2 n^2 \qquad (4)$$

was used instead of the Guinier approximation. The calculated particle sizes agreed within 10% with those obtained by using the Guinier approximation.

In case N(r) is a Maxwellian distribution, $N(r) = r^n e^{-(r/r_0)^2}$ where r_0 and n are constants.

If one writes for a spheroid: $V(r) = (4\pi/3)vr^3$, where v is the axial ratio, and substitutes into the scattering intensity integral, the integral can readily be evaluated at three different limits. For spherical particles v = 1, for disc-shaped particles $v \to 0$, and for rod-like particles $v \to \infty$ and $r \to 0$ simultaneously so the product rv approaches L, the length of a rod with negligibly small radius. Expanding the integral by hypergeometric functions [see Roess and Shull[21]] one gets the scattering from a distribution of particles by different shapes.

By comparison of the experimental data with the theoretical scattering curves, one should be able to get a distribution of the scattering particles and find some information about the general shape of the particles. There are various ways of making graphical comparisons of the data with the theories, one convenient type of plot being that of log $i\theta^2$ vs. log θ^2, which gives curves with distinct maxima on which the effects of shape and

distribution function are fairly readily discernible. In Fig. 3 are plotted the scattering curves for monodisperse spheres and for various Maxwellian distributions. Scattering curves for discs and for rods are also available.[19,21]

The experimental scattering data for platinum on alumina were examined in the light of these theoretical curves, and such conclusions as could be drawn will be taken up with the subsequent discussion of the experimental results.

V. Small Angle X-Ray Scattering Study Of Alumina Supported Platinum Catalysts

There is a major practical difficulty in the small-angle investigation of microporous catalysts, namely, the intense scattering arising from the holes in the catalyst support itself. Consider, for example, the metallized catalyst used in the present investigation, platinum supported on η-alumina. The electron density of platinum is 78X21.45/195.09 = 8.58 faradays per cc; of the crystallites of η-alumina approximately 30X3.7/60 = 1.85 faradays per cc; and of the holes very nearly zero. Since the absolute intensity of the x-ray scattering is proportional to the square of the difference in electron density, a given volume of holes will scatter about 1/13 the intensity of the same volume of platinum. The scattering from holes is easily large enough to permit the small-angle investigation of the particle sizes in the microporous solids themselves, and there are a number of examples in the literature of studies on finely divided solids, including catalysts.[1] Even much smaller differences in electron density are sufficient for small-angle scattering:[5] (0.05 faradays/cc).

If the location of the holes were random with respect to the platinum particles, the scattering from the holes could be treated as part of the background correction and subtracted out. But the platinum particles are sitting within the holes, so that their scattering tends to cancel one another. In fact, our preliminary experiments showed that the scattering from platinum-alumina was apparently less than that from the alumina itself. It is therefore essential to destroy the holes before studying the scattering from the platinum.

A possible method would be to fill the holes with a liquid of the same electron density as the alumina, namely 1.85 faradays per cc. It has been shown[23] that the hole scattering from a silica-alumina cracking catalyst of electron density 1.245 was diminished about two-fold by saturating it with o-xylene, and diminished more than a hundred-fold by saturating it with n-butyl iodide. We have found a better and simpler method to eliminate scattering from the holes.

We have found that by pressing the supported catalysts samples in a hydrostatic press[24] under a pressure of 100 kbar or more, substantially all holes in the alumina are reduced to a size giving no small-angle scattering; the gases originally present escape through the material of the press. In the "pressure sintered" sample the scattering by the metal particles is readily measured.

With the development of pressure sintering as a method for the elimination of hole scattering, it becomes possible to study the effect of such variables as the method of original impregnation, the thermal history of the metallized catalyst, or the chemical attack upon the metal particles. In the present investigation the second of these problems was attacked, namely, the effect of thermal history on particle size. The catalyst chosen for investigation was platinum on alumina. It has been

possible to follow the growth of the platinum particles and to derive information about the kinetics and mechanism of the process.

A. Experimental

The catalysts subjected to study were 5% and 0.5% platinum by weight, dispersed on high-area microporous alumina. The alumina is characterized by its x-ray diffraction pattern as η-alumina; its crystal structure is not affected by heating to the temperatures used in this investigation, and x-ray diffraction patterns taken on our samples after pressure-sintering showed no change in its crystal structure even after compression to 350,000 atmospheres. The catalyst pellets were ground and screened through a 200 mesh/inch screen. The the samples were heat treated (at 400-700°C) for the desired time (1-96 hours) in an oxidizing atmosphere (air) or a reducing atmosphere (generally illuminating gas, but identical results were obtained with hydrogen).

Every time a platinum-alumina sample was heated, a sample of the pure alumina was heated side by side in the furnace, so that a correction might be made in the x-ray measurement for any changes taking place in the "blank" alumina upon heating. In fact this precaution proved to be unnecessary, since all the alumina samples turned out to give identical x-ray scattering. After heat treatment, the platinum-alumina samples were compressed at 100,000 atmospheres for 15 minutes. The detailed description of the high-pressure press is published elsewhere.[24]

Figure 4 shows the x-ray scattering intensity of unheated pure alumina, treated at various pressures. As it shows, the scattering from holes in the alumina has been substantially eliminated at 100,000 atmospheres so this pressure was chosen for the treatment of all samples. Heating in the range of temperatures used has a negligible effect on the compressibility characteristics of the alumina.

There was no change in the shape of the platinum particles due to compression in the pressure range 5-200 kbars, as was determined from the small-angle x-ray scattering data.

At one stage of the investigation an attempt was made to pressure sinter the platinum-alumina first, then heat treat it. The results were quite disconcerting and the attempt was abandoned: the scattering in the small-angle region increase enormously, producing a background scattering so high that the scattering from the platinum particles could not be determined with any confidence. The cause of this phenomenon is the high strain to which the alumina is subjected upon compression, which greatly facilitates crystallization. It is probable that the grains rearrange to an order such as they had before compression, thereby introducing a number of holes.

B. Results and Discussion

1. Growth of Platinum Particles. The body of our platinum-alumina studies were made with 5% platinum catalysts although 0.5% platinum is also easily detectable by its scattering.[19] The samples were compressed at 100,000 atm after the heat treatments.

Figure 5 shows the particle size changes in a reducing atmosphere at two temperatures, 600°C and 700°C and Fig. 6 shows the particle size changes for oxidizing atmospheric heating.

The effect of heat treatment on the particle size is clearly indicated in these data. There is a large increase in the average particle size at these temperatures in the measured time interval. All samples exhibit a very fast growth in the first few hours, which levels off with time. In reducing atmospheric heating, this leveling off or almost complete stop of the growing process is quite conspicuous. In either reducing or oxidizing

atmosphere, a faster change is taking place at the higher temperature. Moreover, it is apparent from the figures that heating in oxidizing atmosphere brings about a very much faster growth process than does heat treatment in reducing atmosphere.

The absolute intensity of scattering (which is proportional to the number of particles whose scattering is detectable) is at first low, increases with heating time, then eventually falls somewhat with long heating times.[19] The plainest interpretation is that at first many particles are too small to be within the range of detection by the x-ray method, as heating progresses they grow larger and become detectable, and at very long times a number of them have become too large to be detectable, their scattering being hidden under the primary beam. In other words, there is no limiting particle size, but a steady transport of material from small particles to larger ones.

The apparent activation energy can be calculated by comparing the elapsed times for a particle to attain a given radius, at two or more temperatures, vis.,

$$E_{activation} = R \; d \ln t_r / d(1/T) \qquad (5)$$

where t_r is the time to attain a given radius.

The apparent activation energy, computed on the foregoing basis, is roughly 20 kcal for a reducing atmosphere and roughly 52 kcal for an oxidizing atmosphere. It is evident that two quite different mechanisms are involved, and tempting to ascribe the low-energy process to some sort of diffusion mechanism and the high energy process to the transport through the gas phase by platinum oxide. From the work of Brewer and Elliot[25] the heat of the reaction $Pt + O_2 = PtO_2(g)$ is $\Delta H = +55$ kcal, so the transport by gaseous PtO_2 becomes plausible. However, it is necessary to

point out that the apparent activation energy may be relatively unreliable as a measure of the true activation energy, because as we shall show, the radius-dependence is itself highly temperature dependent.

The growth or precipitation of particles in a solid matrix, far from equilibrium, proceeds at a constant, mostly volumetric rate[26,27] $r^2 dr/dt = k$. Here, k is the rate constant. This equation applies to relatively large particle (1 micron or more). Small particles in the 10Å to 10^3Å range due to their increased surface energy have solubilities larger than that of the large particles as expressed by the Thompson equation,[28]

$$\ln C_r/C_s = 2V\gamma/rRT \qquad (6)$$

Here, C_r is the solubility of particles of radius r, and C_s is the limiting solubility for large particles, V is the molar volume, γ is the surface tension of the particle in the solid matrix, R is the gas constant and T is the absolute temperature. Therefore the rate of growth of larger particles as long as small particles are present is accelerated by a factor of $\exp(2V\gamma/rRT)$. Under these conditions the growth law becomes

$$r^2 dr/dt = ke^{a/r} \qquad (7)$$

where $a = 2V\gamma/RT$. It is the presence of the surface energy term which accounts for both the decrease of rate with particle size and the increase of activation energy with particle size.

The variables of Eq. 7 are easily separable and the resulting differential equation has been integrated[19] to give

$$kt/a^3 = (r/a)^4 e^{-a/r} S(a/r) \qquad (8)$$

where the function, $S(a/r)$, can be approximated by the simple equation 6

$$S(a/r) \approx \frac{1+a/r}{a/r+5+3(r/a)} \qquad (9)$$

It is worth commenting that the theoretical curve is almost linear when r is plotted against log t as long as the growth is controlled by the surface energy term.

The fitting of experimental data to the theoretical curves requires knowledge of the parameters a and k. This can be accomplished by trial in a variety of ways; perhaps the simplest is to plot $\log(t/r^4 S)$ against $1/r$, from which the slope gives a and the intercept gives ka. This kind of plot must be iterated, since S is a function of a/r and requires a prior knowledge of a; however, S is a slowly varying function and an approximate preliminary value of a permits it to be evaluated rather well.[19]

The lines drawn through the data points on Figs. 7 and 8 were calculated from the theoretical equation with the foregoing parameters.[19] Except for the very shortest times, the agreement is within our experimental error.

The explanation for the great deviation at very short times is that it probably does not represent a real growth of (arithmetic mean) particle size at all, but represents a change in the distribution function of particles, toward a broader distribution. As we shall give evidence to show later, the initial metal particles are fairly near to monodisperse, but rapidly change to a rather broad distribution. Since, as we have pointed out, the x-ray method looks at particles considerably larger than the average particles, the change in distribution will simulate the growth

of particle size.

The rate constant k for a reducing atmosphere is given approximately by $5X10^8$ exp(-38,000/RT) and for an oxidizing atmosphere by $2.51X10^{17}$ exp(-69,000/RT) $Å^3$/hr. These activation energies would be the true activation energies for the transport in contact with bulk material, or very large particles. It is clear from the numbers that the two processes, reducing and oxidizing atmosphere growths, are very different. However, there is a rather large possible error in the numerical values and it would be unsafe to draw mechanistic conclusions from their values.

b. The Size Distribution and Shape of Particles. In order to examine the distribution and shape characteristics of the platinum particles, the data have been replotted as log $i\theta^2$ vs. log θ^2, to give the same kinds of graphs as were discussed above. Representative curves are displayed in Figs. 9 and 10.

The dotted curves on the figures correspond to the platinum in the unheated samples. As a comparison with the theoretical curve will easily show, these correspond rather well to the curve for monodisperse spheres; so it is a good approximation that the freshly deposited platinum is made up of spherical particles with a narrow distribution range.

Upon heat treatment of the samples, the scattering curves become progressively flatter, indicating a broad distribution of sizes. As time goes on, the intensity at large angles diminishes and at small angles grows, which of course indicates that smaller particles are disappearing while large particles are growing. The curves are similar in shape to those for a Maxwellian distribution of spheres with n = 3 or less in N(r).

The very flat distribution is particularly noticeable in the data for an oxidizing atmosphere. The theoretical curves for a flat distribution

of spheres are rather similar to those for a distribution of discs, and it is not possible to make a firm decision as to the shape. It is not implausible that in the oxidizing atmosphere the particles redeposit on the alumina in a somewhat plate-like form, since platinum oxide may well be able to wet alumina.

ACKNOWLEDGEMENTS

This work was performed under the auspices of the United States Atomic Energy Commission.

Table I. List of Surface Structures Which Were Detected on the Different Low Index Surfaces of Platinum and Their Approximate Temperature Range of Stability

Substrate	Surface Structure	Approximate Temperature Range of Stability
Pt (100)	(5x1)	350-500°C
	(2x1)	300-500°C
	⊙ [a]	> 700°C
Pt (100)	⊙ [a]	> 600°C
Pt (111)	(2x2)	800-1000°C
	(3x3)	800-1000°C
	⊙ [a]	> 900°C

[a] The notation, ⊙, indicates a ring-like diffraction pattern.

References

1. A. Guinier and G. Fournet, "Small-Angle Scattering of X-Rays," pp. 187-194, John Wiley and Sons, New York (1955).
2. J. A. Simpson, Rev. Sci. Instr. 35, 1698 (1964).
3. C. W. Caldwell, Jr., Rev. Sci. Instr. 36, 1500 (1965).
4. B. K. Vainshtein, "Structure Analysis by Electron Diffraction," Pergamon Press, New York (1964).
5. J. J. Lander, "Progress in Solid State Chemistry," (H. Reiss, ed.) Pergamon Press, New York (1965).
6. A. Chutjian and G. A. Somorjai, to be published.
7. R. E. Schlier and H. E. Farnsworth, "Semiconductor Surface Physics," University of Pennsylvania Press, Philadelphia (1956).
8. A. U. MacRae, Surface Sci. 4, 247 (1966).
9. N. A. Gjostein, "Metal Surfaces," Chapter IV, American Society for Metals 1963.
10. H. B. Lyon and G. A. Somorjai, J. Chem. Phys. 44, 3707 (1966).
11. B. C. Clark, R. Herman, and R. F. Wallis, Phys. Rev. 139, A860 (1965).
12. A. U. MacRae and L. H. Germer, Ann. N. Y. Acad. Sci. 101, 627 (1963).
13. L. G. Feinstein and D. P.Shoemaker, Surface Sci. 3, 294 (1965).
14. G. A. Somorjai, A. Chutjian and A. M. Mattera, Bull. Am. Phys. Soc. 11, 727 (1966).
15. A. M. Mattera, R. M. Goodman and G. A. Somorjai, Surface Science (April 1967, to be published).
16. H. A. Levy, P. A. Agron, M. A. Bredig, and M. D. Danford, Ann. N. Y. Acad. Sci. 79, 762 (1960).
17. N. W. Gingrich, "Liquids; Structure, Properties, Solid Interactions," (T. J. Hughel, ed.), Elsevier Publishing Co., New York (1965).
18. H. B. Lyon and G. A. Somorjai, J. Chem. Phys. 1967, to be published.

19. G. A. Somorjai, (Ph. D. Thesis), University of California (1960).

20. W. Parrish and T. R. Kohler, Rev. Sci. Instr. 27, 795 (1956).

21. L. C. Roess and C. G. Shull, J. Appl. Phys. 18, 295 (1947).

22. E. A. Porai-Koshits and L. S. Andreyev, J. Soc. Glass Tech. 43, 235T (1959).

23. E. L. Gunn, paper presented at the April 1958 meeting of the American Chemical Society, Division of Petroleum Chemistry.

24. P. W. Montgomery, H. Stromberg, and G. Jura, University of California UCRL-9796 (1961).

25. L. Brewer and G. R. Elliott, (Ph. D. Thesis), University of California (1952).

26. F. J. Morin and H. Reiss, J. Phys. Chem. Solids, 3, 196 (1957).

27. G. A. Somorjai, J. Chem. Phys. 35, 655 (1961).

28. H. K. Hardy and T. J. Heal, Progr. Metal Phys. 5, 143 (1954).

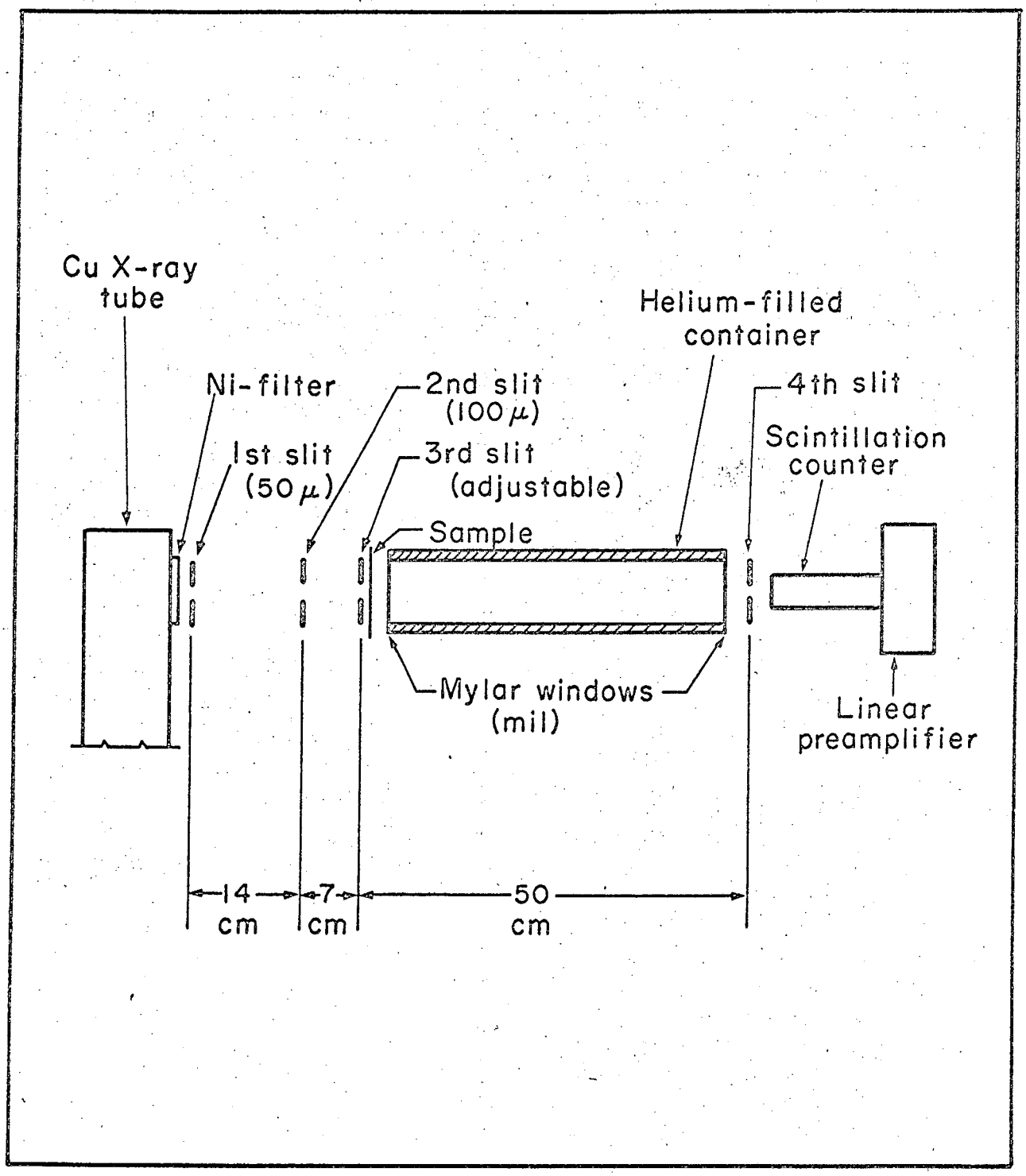

Fig. 1 Scheme of the Low Energy Electron Diffraction experiment.

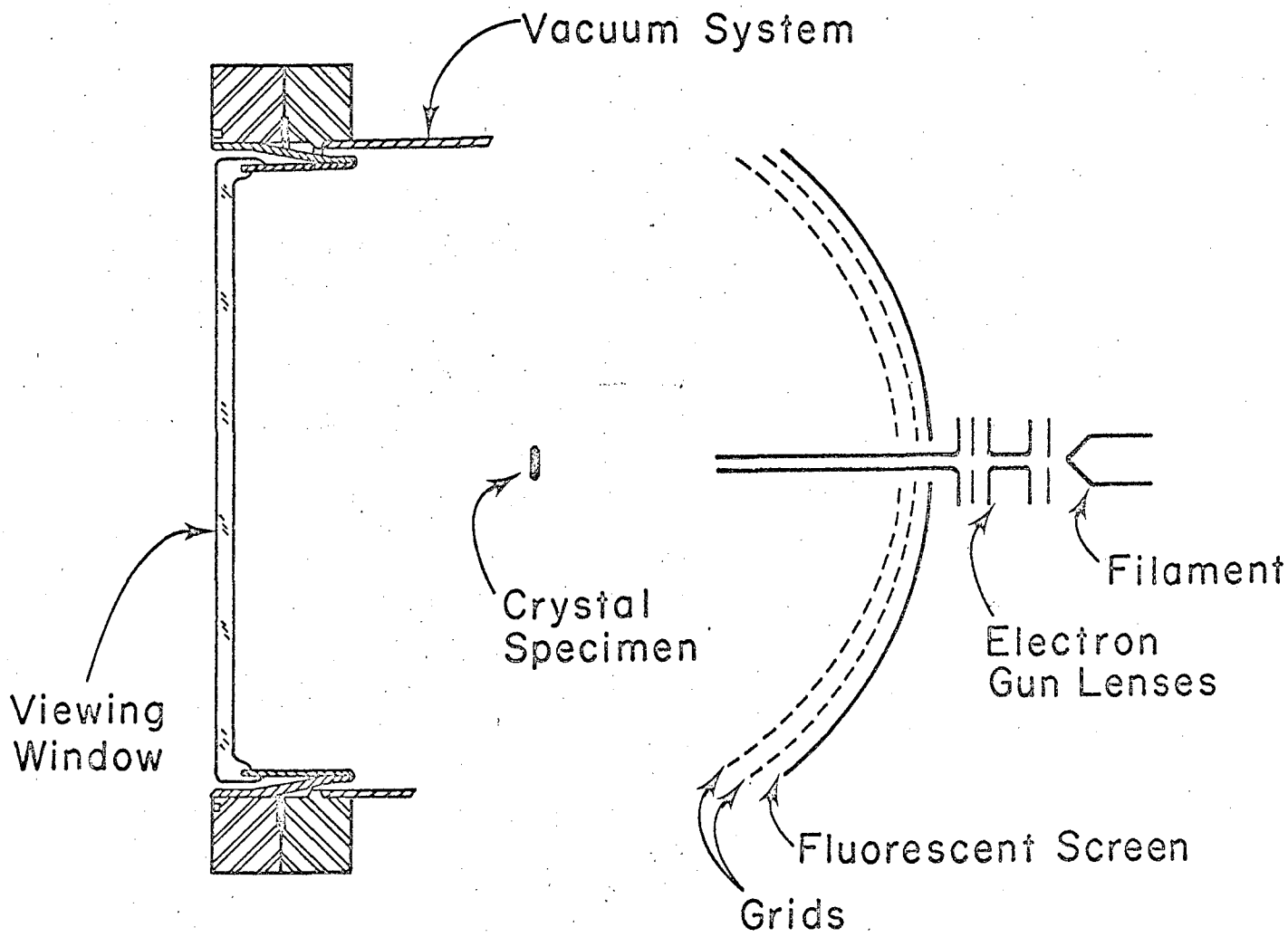

The Diffraction Apparatus

Fig. 2 Scheme of the small angle x-ray scattering experiment.

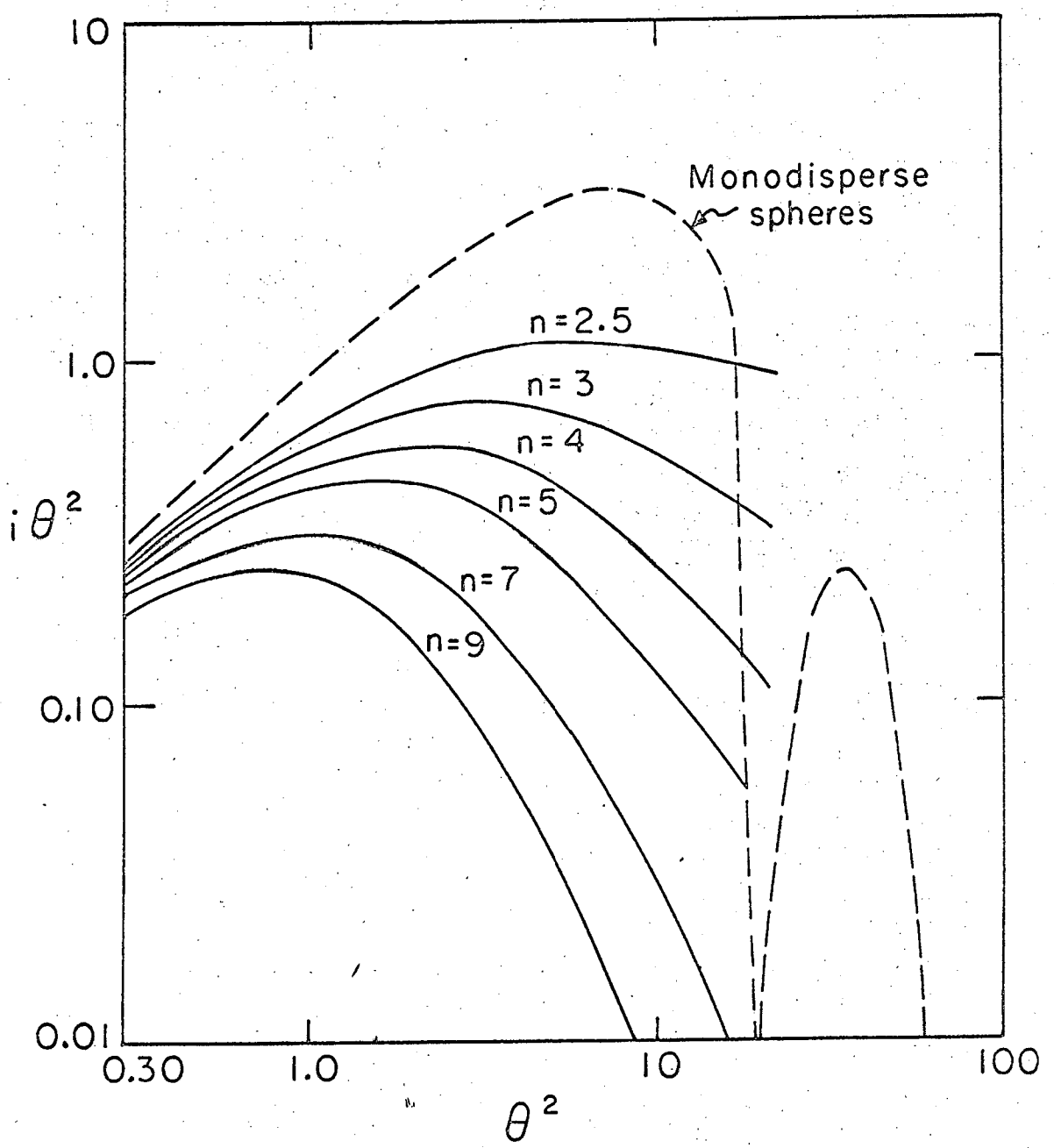

MUB-6528

Fig. 3 Scattering curves for monodisperse spheres and Maxwellian. Distribution of heterodisperse spheres.---Monodisperse spheres.

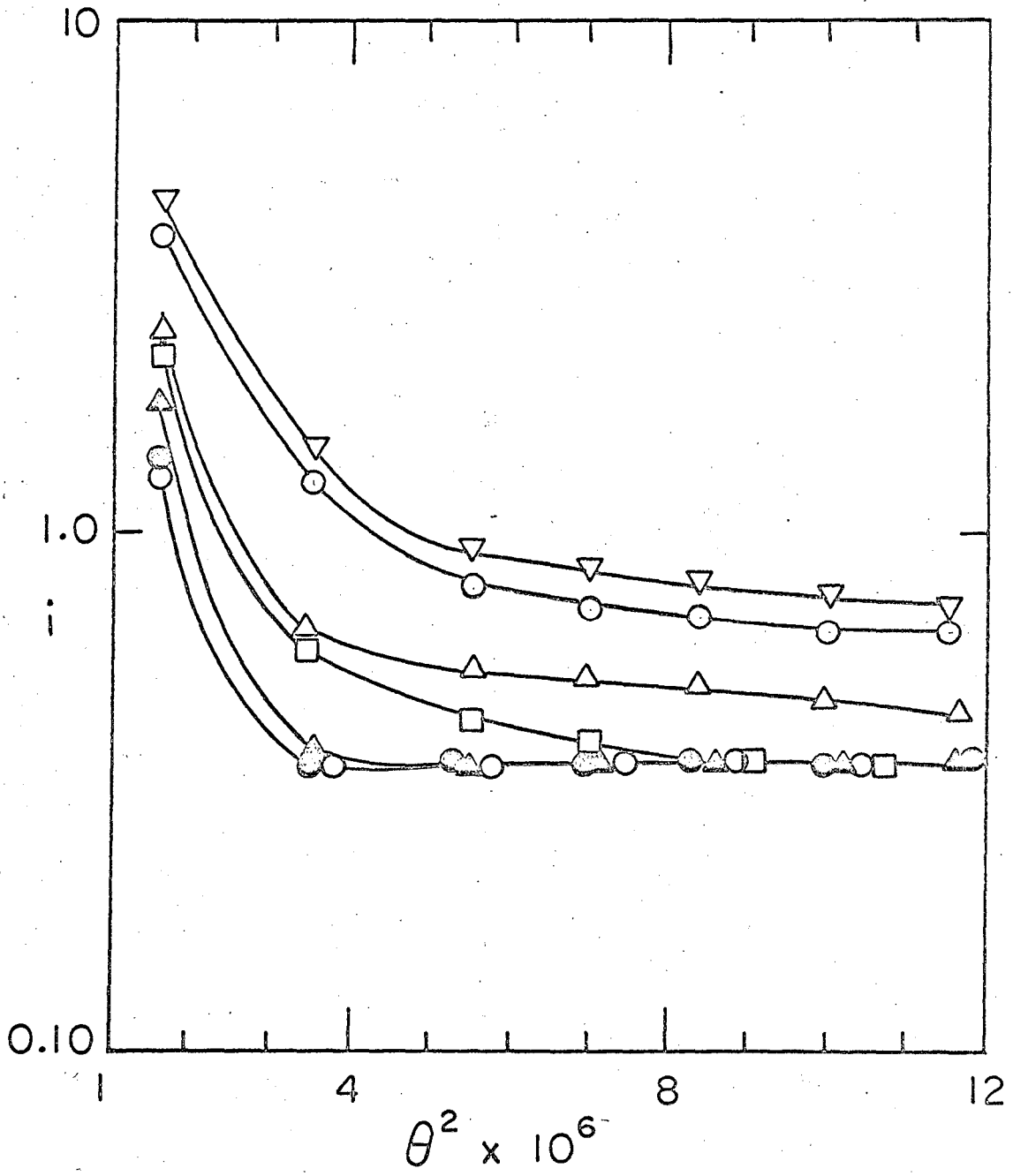

MUB-6527

Fig. 4 Scattering intensity of unheated η-alumina at various pressures. i: Intensity in units of 256 counts/30 sec. θ: Angle in radians. ● air background alone, no sample, ▲ alumina pressed at 100,000 atm., O alumina pressed at 300,000 atm., □ alumina pressed at 65,000 atm., △ alumina pressed at 40,000 atm., O alumina pressed at 20,000 atm., and ▽ alumina unpressed.

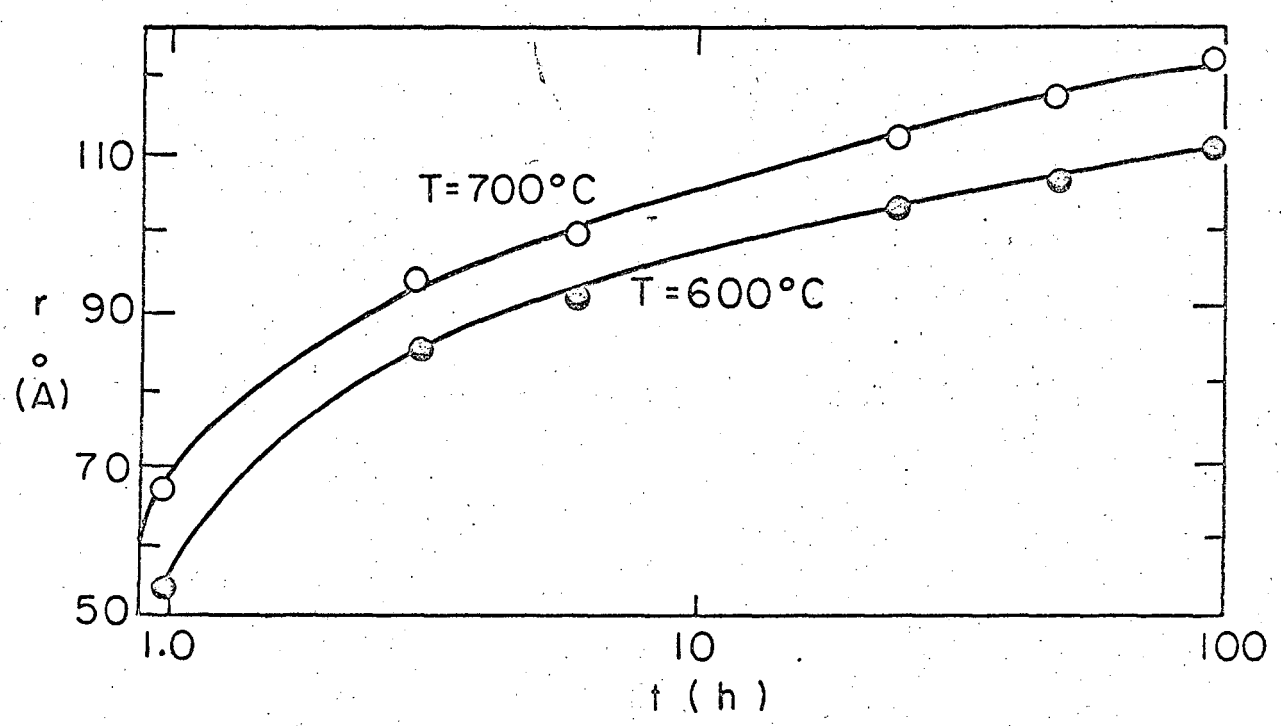

MUB-6531

Fig. 5 Change of the platinum particle size as a function of heating time in reducing atmosphere.

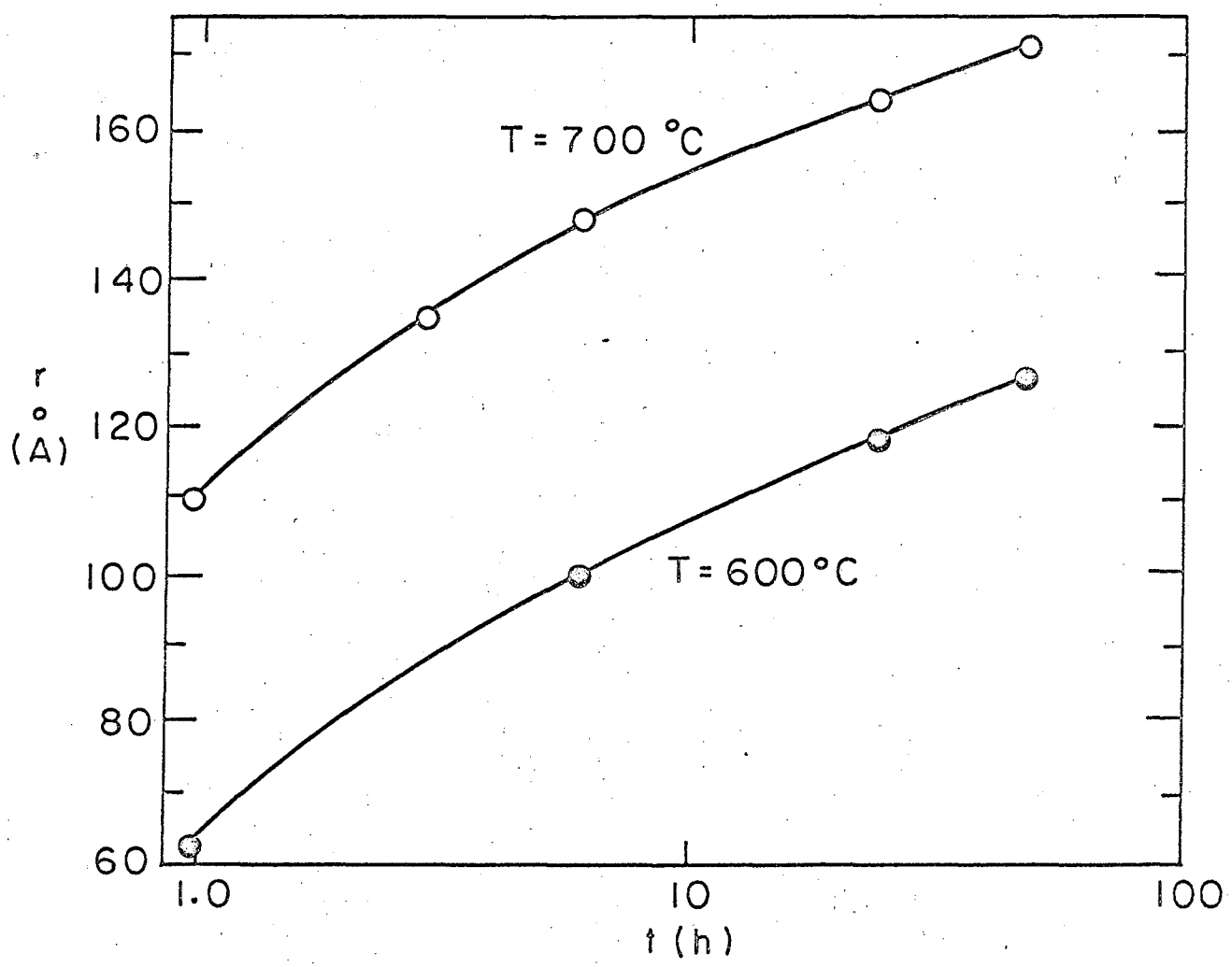

MUB-6532

Fig. 6 Change in the platinum particle size as a function of heating time in oxidizing atmosphere.

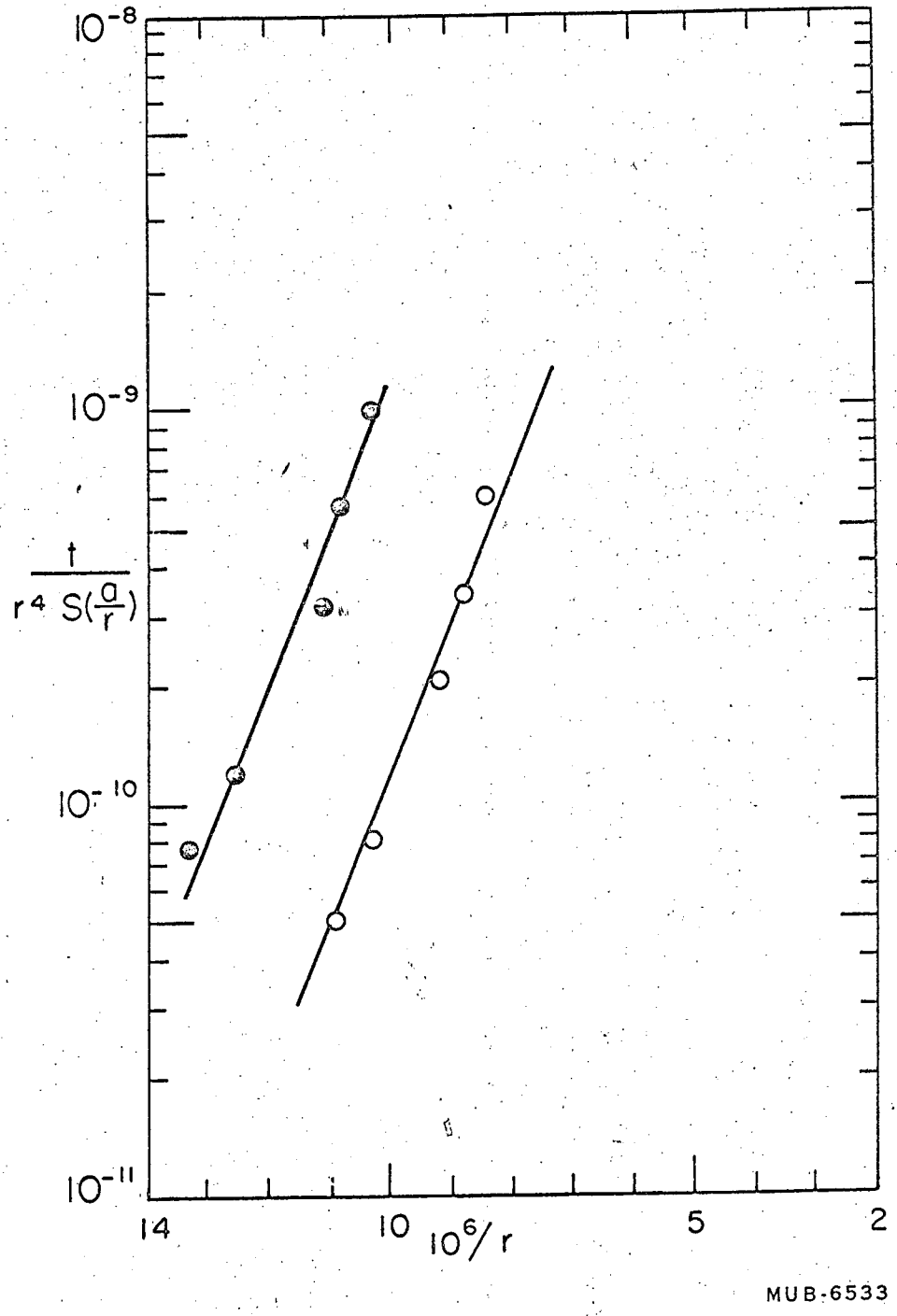

Fig. 7 A plot of the change of the radius of gyration, r, as a function of time for heat treatment at ● - 600°C reducing atmosphere and O - 700°C reducing atmosphere.

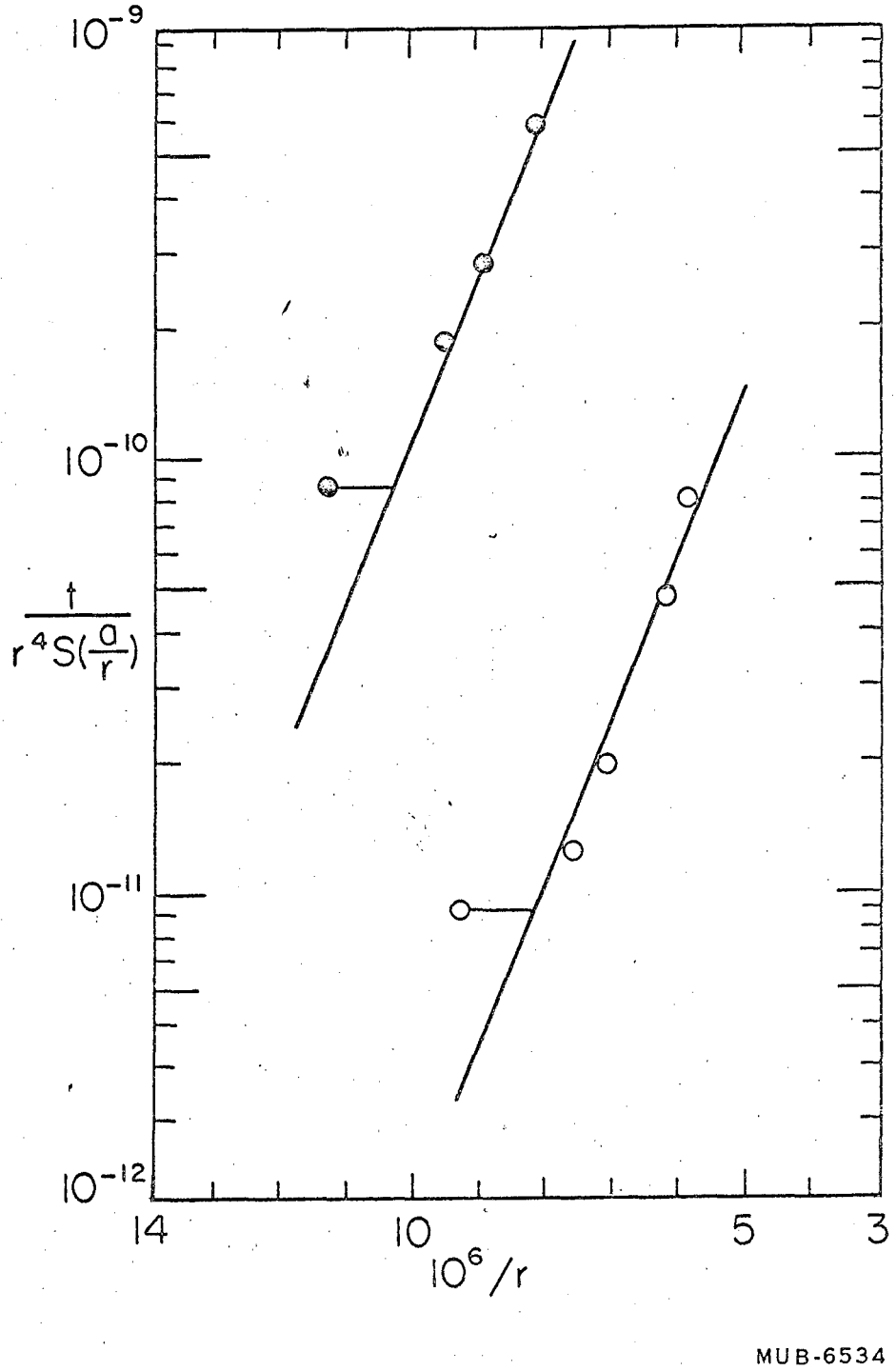

Fig. 8 A plot of the change of the radius of gyration, r, as a function of time for heat treatment at ● 600°C oxidizing atmosphere and O 700°C oxidizing atmosphere.

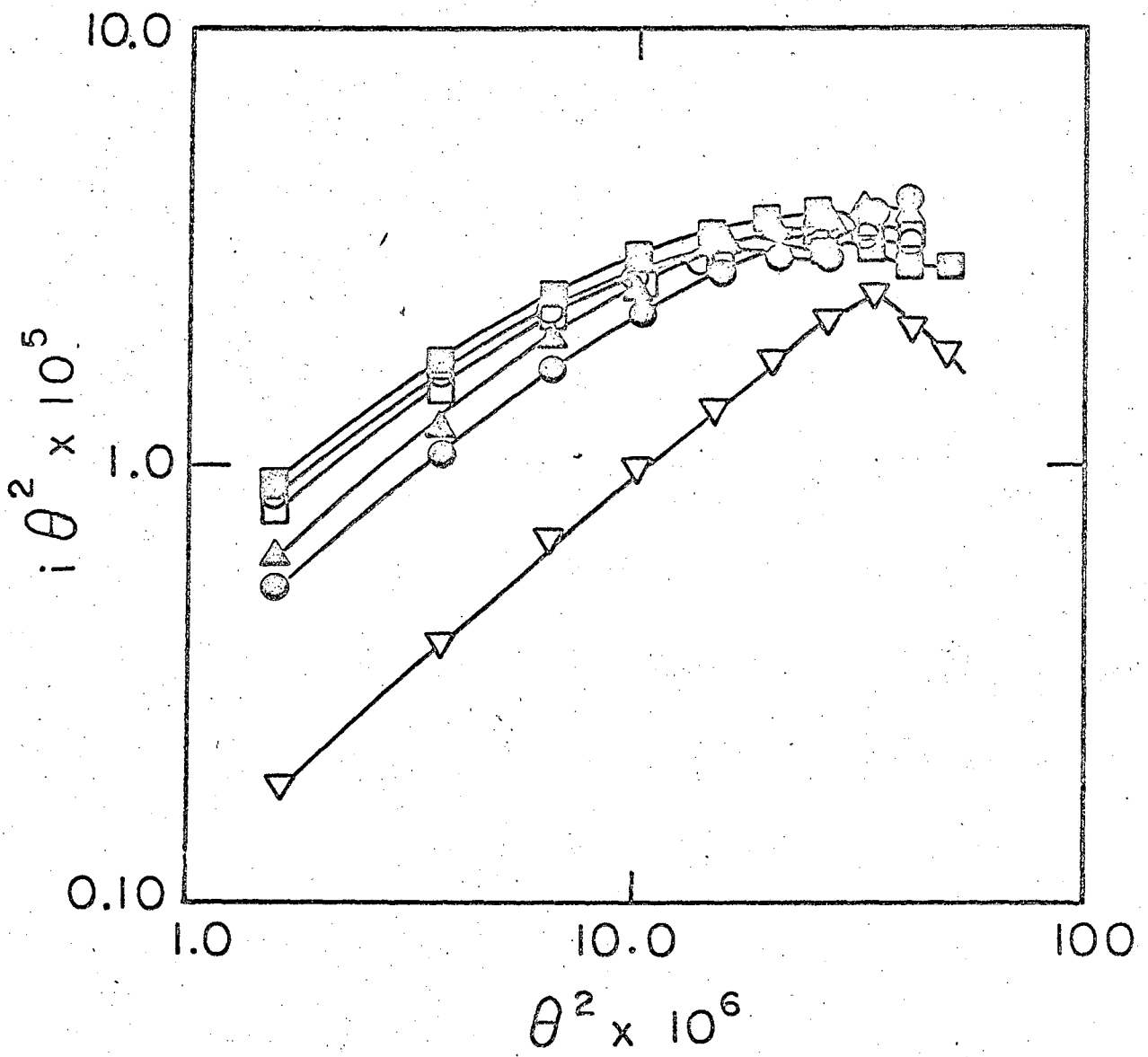

MUB-6535

Fig. 9 5% platinum on alumina, 600°C in reducing atmosphere. ▽ heated for 1 hour or unheated, ● heated for 3 hours, ▲ heated for 6 hours, □ heated for 24 hours, ○ heated for 48 hours, ■ heated for 96 hours.

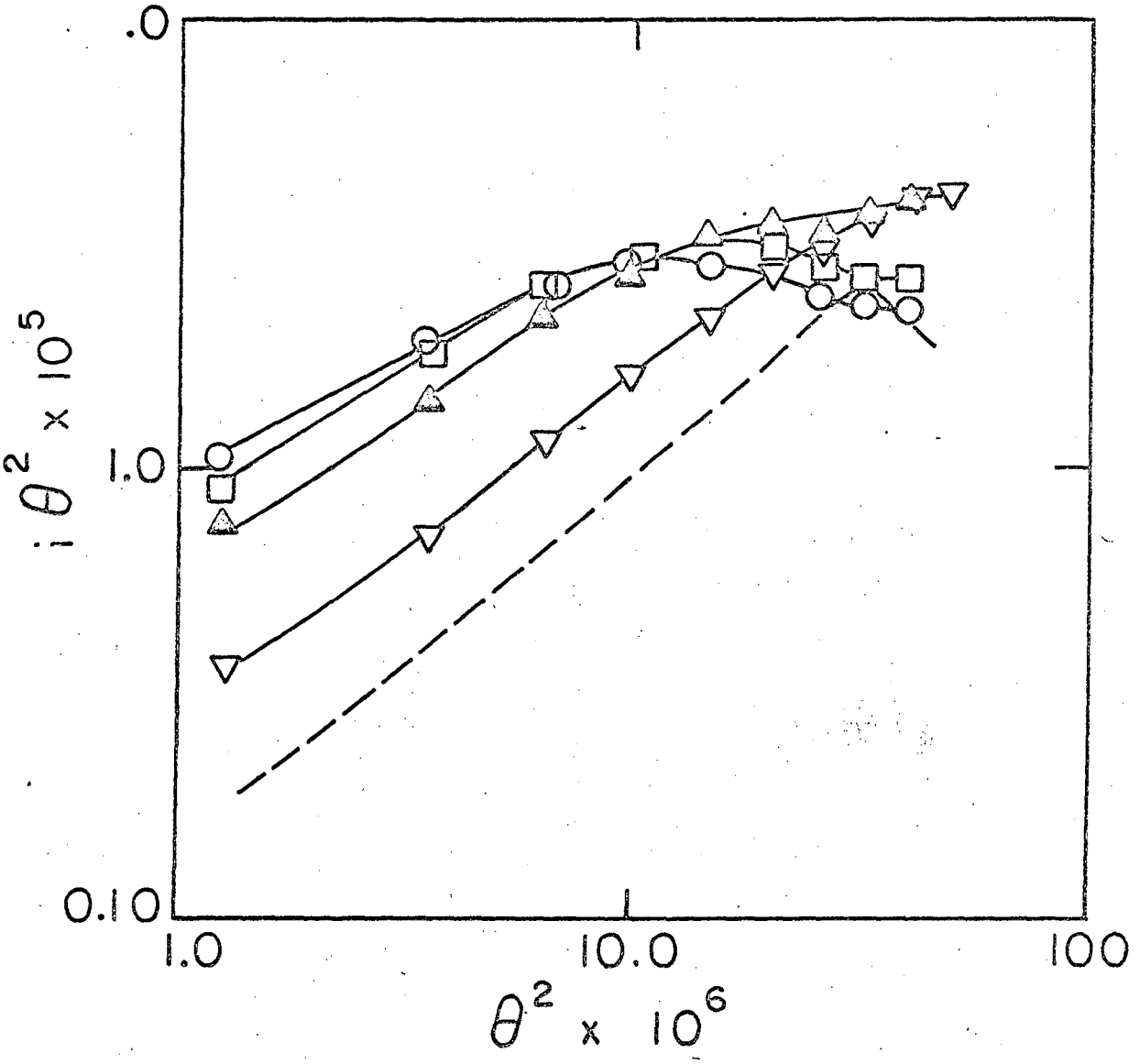

MUB-6537

Fig. 10 5% platinum on alumina, 600 °C in oxidizing atmosphere. △ heated for 1 hour, ▲ heated for 6 hours, □ heated for 24 hours, O heated for 48 hours, --- unheated sample.

This report was prepared as an account of Government sponsored work. Neither the United States, nor the Commission, nor any person acting on behalf of the Commission:

A. Makes any warranty or representation, expressed or implied, with respect to the accuracy, completeness, or usefulness of the information contained in this report, or that the use of any information, apparatus, method, or process disclosed in this report may not infringe privately owned rights; or

B. Assumes any liabilities with respect to the use of, or for damages resulting from the use of any information, apparatus, method, or process disclosed in this report.

As used in the above, "person acting on behalf of the Commission" includes any employee or contractor of the Commission, or employee of such contractor, to the extent that such employee or contractor of the Commission, or employee of such contractor prepares, disseminates, or provides access to, any information pursuant to his employment or contract with the Commission, or his employment with such contractor.